 ©2014 Kvantovaya Elektronika and Turpion Ltd

PACS numbers: 42.55.Px; 42.60.By; 42.60.Jf; 42.60.Lh
DOI: 10.1070/QE2014v044n02ABEH015369

Emission parameters and thermal management of single high-power 980-nm laser diodes

V.V. Bezotosnyi, O.N. Krokhin, V.A. Oleshchenko, V.F. Pevtsov, Yu.M. Popov, E.A. Cheshev

Abstract. **We report emission parameters of high-power cw 980-nm laser diodes (LDs) with a stripe contact width of 100 μm. On copper heat sinks of the C-mount type, a reliable output power of 10 W is obtained at a pump current of 10 A. Using a heat flow model derived from analysis of calculated and measured overall efficiencies at pump currents up to 20 A, we examine the possibility of raising the reliable power limit of a modified high-power LD mounted on heat sinks of the F-mount type using submounts with optimised geometric parameters and high thermal conductivity. The possibility of increasing the maximum reliable cw output power to 20 W with the use of similar laser crystals is discussed.**

Keywords: *high-power laser diodes, efficiency, spectrum, C-mount, F-mount, diamond submount.*

The necessity to raise the output power and brightness and ensure high reliability and a long operating life of laser diodes stems from the increasing potential of their emission for direct use in materials processing and other applications [1–3]. This paper presents a continuation of our previous research and design work aimed at solving the problem of increasing the output power, brightness, efficiency and operating life of high-power laser diodes [4–6].

1. Experimental results and calculation of overall efficiency

We present measured output parameters of a 980-nm LD with a stripe contact width of 100 μm and cavity length of 4 mm, mounted on a standard heat sink of the C-mount type in our laboratory. Figure 1 shows the light power–current ($L–I$) curve and the variation of overall efficiency in a wide range of pump currents [from the lasing threshold (0.5 A) to 23 A] for quasi-cw operation of the LD. Since the time needed to measure $L–I$ and current–voltage ($I–V$) characteristics and emission spectra is 1.5 min, steady-state thermal conditions, with thermal equilibrium between all the components of the system, are not reached.

As seen in Fig. 1, in this unsteady-state continuous mode the $L–I$ curve remains linear at currents up to 14 A, whereas at higher currents its slope decreases markedly. The highest overall efficiency (68%) is reached at a pump current of 7 A.

V.V. Bezotosnyi, O.N. Krokhin, V.A. Oleshchenko, V.F. Pevtsov, Yu.M. Popov, E.A. Cheshev P.N. Lebedev Physics Institute, Russian Academy of Sciences, Leninsky prosp. 53, 119991 Moscow, Russia; e-mail: victorbe@sci.lebedev.ru, pvf@sci.lebedev.ru, on-vlad@yandex.ru

Received 18 December 2013
Kvantovaya Elektronika **44** (2) 145–148 (2014)
Translated by O.M. Tsarev

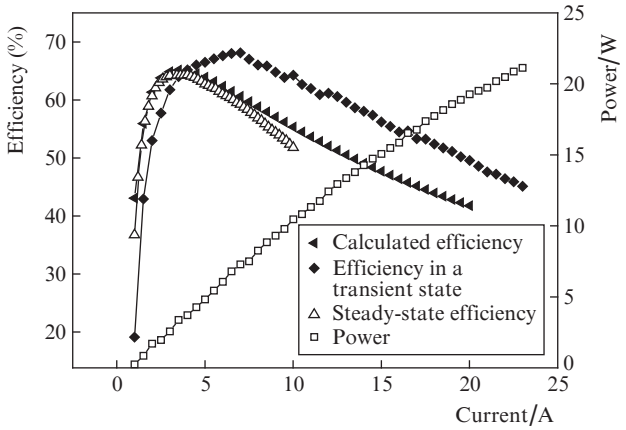

Figure 1. Light power–current curve and overall efficiency of a 980-nm laser diode.

The output power reached 22–23 W and was limited by catastrophic optical failure of the output mirror.

$L–I$ measurements in the temperature range 10–50 °C show that the LDs have sufficient thermal stability. The temperature constants for the threshold current I_{th} (T_0) and efficiency η_d (T_1) evaluated from these data are 175 and 303 K, respectively. At thermal equilibrium, the measured and calculated maximum efficiencies are markedly lower (64% and 65%, respectively) and are reached at pump currents of 4 and 4.5 A. At currents below 7 A, the calculated and experimentally determined values differ insignificantly. At higher pump currents, the measured efficiency is substantially lower, which is attributable to the insufficient heat removal efficiency at high injection levels and the use of a copper C-mount.

Figure 1 demonstrates that, under unsteady-state conditions, an output power of 20 W is reached at a pump current of 23 A. The overall efficiency is then 46%. A more realistic estimate of the overall efficiency at 20-W power was made using temperature-dependent overall efficiency data for steady-state cw operation in comparison with calculation results for currents up to 20 A. At a current of 20 A, the calculated efficiency is 41%; at 23 A, with correction based on experimental data approximation we obtain 35% to 38%. In accordance with this level, we chose the range of thermal loads in modelling the thermal conditions corresponding to an output power of 20 W.

2. Spectral parameters and reliable operation criterion

Figure 2 shows the emission wavelength at the maximum of the spectral envelope, λ_{max}, as a function of pump current

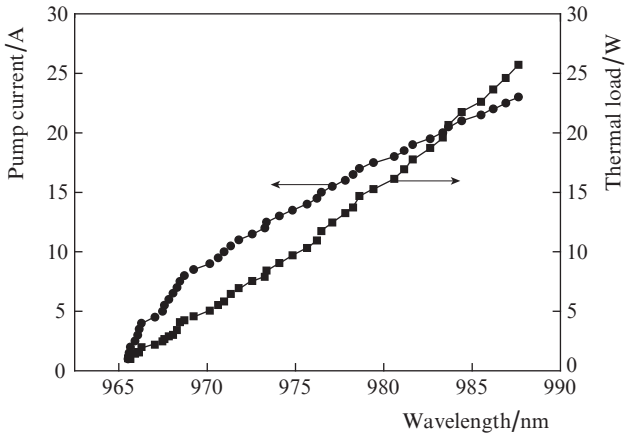

Figure 2. Variation in the wavelength at the maximum of the spectral envelope.

and thermal load P_{therm} determined from experimental pump current I and voltage V data and expressed through the overall efficiency η_{tot}:

$$P_{\text{therm}} = IV(1 - \eta_{\text{tot}}). \quad (1)$$

The $\lambda_{\max}(I)$ curve is superlinear, in accordance with the fact that the Joule loss is a quadratic function of pump current, and $\lambda_{\max}$ is an almost linear function of $P_{\max}$, as expected. The slight deviation from linearity is in part caused by the experimental uncertainty in the position of the maximum in the envelope, which increases with increasing pump current because of the significant broadening of the spectrum and the presence of several (two or three) small peaks at the maximum in the envelope due to the unsteady-state thermal conditions during the measurements. Thus, increasing the pump current from 0.5 to 23 A increases $\lambda_{\max}$ by 25 nm, the estimated overheating of the active region at a current of 23 A is 83 °C, and the temperature of the active region is 103 °C.

It is important to note that, according to our test results, more than 90% of the samples tested were capable of reliably operating at an output power of 10.5 W and only about 50% of the samples withstood 11.5 W power. Thus, the data in Fig. 2 can be used to derive an empirical criterion for long-term stable, reliable continuous operation at a heat sink base temperature of 20 °C: overheating of the active region should not exceed 20–25 °C. According to the data in Fig. 3, the full width at half maximum of the spectral envelope, $\Delta\lambda_{\max}$, in the range of pump currents in question increases by almost a factor of 5: from 1.1 to 5.2 nm. One interesting feature of the data is that the spectral width is a nonmonotonic function of pump current: it has peaks at rather regular intervals. One possible reason for this is that, in our measurements, the pump current was increased stepwise and, as a consequence, thermal equilibrium was reached in an oscillatory way. Somewhat nonmonotonic behaviour of $\Delta\lambda_{\max}(I)$ was also observed under steady-state conditions, but the separation between and the height of the peaks obtained at varied pump current were several times smaller.

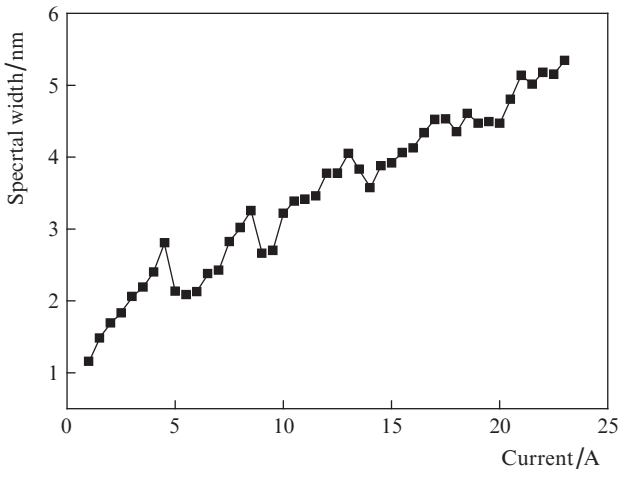

Figure 3. Full width at half maximum of the envelope of the emission spectrum vs. pump current.

3. Modelling of heat flows and optimisation of parameters of submounts

Thermal management is a key issue in the case of high-power laser diodes, along with the optical damage resistance of their mirrors. Thermal management has been the subject of many studies (see e.g. Refs [7–11]). In contrast to previous work [10, 11], heat flows were modelled in this study in three dimensions, which allowed us to obtain temperature profiles along all coordinate axes and examine the effects of the geometric parameters of the system, materials and thermal load P_{therm} [see (1)].

The reference P_{therm} values used to model thermal conditions were dictated by the necessity to develop a more efficient high-power LD design that would allow the reliable power limit to be raised from 10 (for LD chips on a copper C-mount) to 20 W (for a new heat sink design at the same laser crystal parameters). Conceptual feasibility of reliable operation of a 980-nm LD at an output power near 20 W was demonstrated by mounting a laser crystal using a copper–diamond composite submount [1]. Unfortunately, LD operation at temperatures below the dew point is hindered in practice, because an isolated chamber with a certain medium is needed to prevent condensation. In view of this, we modelled the possibility of reliable operation at a heat sink base temperature of 20 °C.

Mounting on copper C-mounts ensured a reliable output power limit of 10 W at an overall efficiency of 50%, stripe contact width of 100 μm and cavity length of 4 mm. The heat flux density was then 2.5 kW cm^{-2}. According to our estimates, when the output power is increased to 20 W, it is necessary to remove a continuous heat flux with a density of 7.5–10 kW cm^{-2}.

This continuous heat flux density is extremely high. Heat fluxes are even more difficult to remove in the case of LDs because parameters of a laser crystal produced from a semiconductor heterostructure are strong functions of temperature and, as pointed out above, overheating of the active region should not exceed 20–25 °C.

Heat flows were modelled for an LD design based on a standard basic heat sink of the F-mount type, more efficient than the C-mount, using submounts with high thermal conductivity (the range of thermal conductivity values used in modelling corresponds to synthetic diamond [5]). The modelling results are presented in Figs 4 and 5.

Figure 4 shows the calculated temperatures at the output and (high-reflectivity) back mirrors and the average temperature of the active layer along the length of the crystal as functions of thermal load for a basic heat sink of the F-mount type with no submount and with a diamond submount having a thermal conductivity of 1200 W m^{-1} K^{-1}. The dimensions of the submount – 0.3 mm thickness, 2 mm width and 4.2 mm length – are identical to those used in previous experiments [5]. As seen in Fig. 4, at a thermal load of 35 W the temperature difference across the active region along the length of the cavity, $\Delta T = T_{M1} - T_{M2}$, is 16.5 °C with no submount and 2.5 °C when a diamond submount is used. The average temperatures of the active region, T_m, without and with a submount are 54 and 48 °C, respectively. Note that T_m is closer to T_{M1} with no submount and to T_{M2} when a submount is used. This example demonstrates that, when the thermal conductivity of a submount having far-from-optimal parameters is sufficiently high, the negative thermal lensing effect compensates the additional thermal resistance due to the thickness of the submount and it allows one not only to reduce the absolute temperature of the active region but also to considerably decrease the temperature difference along the length of the crystal, which should have an advantageous effect on the output power level, the width of the emission spectrum and the reliability and operating life of high-power lasers.

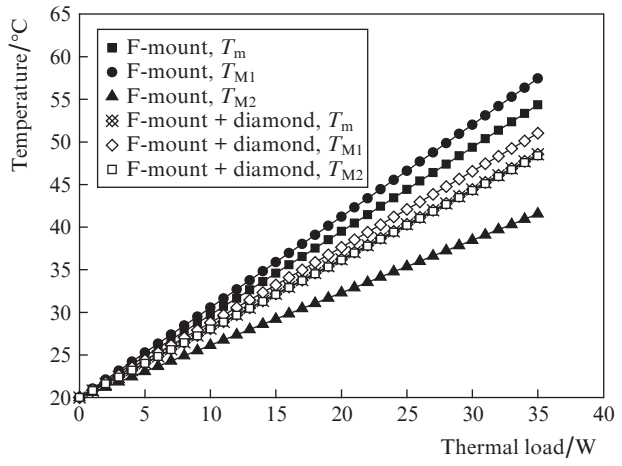

Figure 4. Calculated temperatures vs. thermal load for LD crystals on an F-mount. T_m is the average temperature of the active region along the length of the crystal, and T_{M1} and T_{M2} are the temperatures of the active region at the output and (high-reflectivity) back mirrors, respectively.

Optimisation of submount dimensions allows one to reduce the average temperature of the active region of the LD (Fig. 5). The minima in T_m calculated for a thermal load of 35 W and submount widths of 2 and 4 mm are due to heat spreading over the width of the submount. It is seen that, at a thermal conductivity of 1200 W m^{-1} K^{-1}, the above reliable operation criterion corresponds to a submount more than 0.4 mm thick and 6 mm wide. The thicker the diamond, the more efficient is the heat removal. In an ideal case, this would allow one to dispense with a basic copper F-mount having a high thermal resistance. The use of diamond submounts more than 1 mm in thickness and more than 4 mm in width, with a thermal load conductivity above 2000 W m^{-1} K^{-1} offers the possibility of considerably lowering the temperature of the active layer. Unfortunately, increasing the volume of diamond

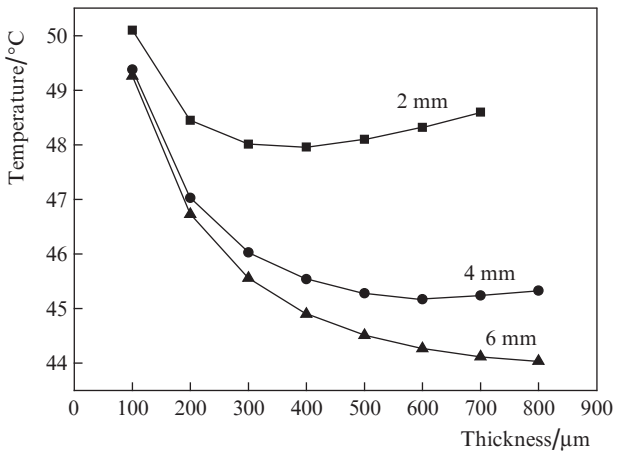

Figure 5. Average active-region temperature as a function of the thickness of diamond submounts 2, 4 and 6 mm wide. Modelling was carried out at a thermal load of 35 W and a submount thermal conductivity of 1200 W m^{-1} K^{-1}.

submounts poses great technical problems pertaining to the growth of thick plates and, accordingly, increases their cost. Nevertheless, the use of such large and expensive diamond elements for reaching extreme power and brightness levels is justified in a number of cases. Moreover, increasing the submount dimensions makes it necessary to develop and optimise new types of basic heat sink, with large dimensions.

4. Conclusions

Several groups of 980-nm laser diodes (about 70 devices) on copper C-mounts have been fabricated and their optical emission properties, electrical characteristics and reliability limits have been investigated in a wide range of pump currents. We have achieved an overall efficiency as high as 65% and high uniformity of LD parameters within a given group, with a 10 W cw output power and 90% yield after life tests. We have determined the overall efficiency as a function of pump current, compared the data to calculation results and estimated the thermal load at a calculated cw output power of 20 W. From spectral characteristics and reliability limits, we have derived a criterion for reliable continuous operation at an F-mount backside temperature of 20 °C. We have performed three-dimensional modelling of heat flows in a laser crystal mounted on a copper heat sink with a synthetic diamond submount and examined the effect of the geometry and thermal conductivity of diamond submounts on the maximum reliable power of LDs.

Acknowledgements. We are deeply grateful to V.I. Konov, V.G. Ral'chenko, E.E. Ashkinazi and A.F. Popovich (A.M. Prokhorov General Physics Institute, Russian Academy of Sciences) for providing the diamond samples and for useful information and fruitful discussions.

This work was supported by the Presidium of the Russian Academy of Sciences (Programme No. 7OF).

References

1. Crump P., Blume G., Paschke K., Staske R., Pietrzak A., Zeimer U., Einfeldt S., Ginolas A., Bugge F., Häusler K., Ressel P., Wenzel H., Erbert G. *Proc. SPIE Int. Soc. Opt. Eng.*, **7198**, 719814-1 (2012).

2. Sin Y., LaLumondiere S.D., Presser N., Foran B.J., Ives N.A., Lotshaw W.T., Moss S.C. *Proc. SPIE Int. Soc. Opt. Eng.*, **8241**, 824116-1 (2012).
3. Yanson D., Cohen S., Levy M., Shamay M., Geva A., Berk Y., Tesler R., Klumel G., Rappaport N., Karni Y. *Proc. SPIE Int. Soc. Opt. Eng*., **8640**, 86401I-1 (2013).
4. Ashkinazi E.E., Bezotosnyi V.V., Bondarev V.Yu., Kovalenko V.I., Krokhin O.N., Oleshchenko V.A., Pevtsov V.F., Popov Yu.M., Cheshev E.A., in *Poluprovodnikovye lazery i sistemy na ikh osnove* (Semiconductor Lasers and Related Systems) (Minsk: IF NANB, 2011) p. 29.
5. Ashkinazi E.E., Bezotosnyi V.V., Bondarev V.Yu., Kovalenko V.I., Konov V.I., Krokhin O.N., Oleshchenko V.A., Pevtsov V.F., Popov Yu.M., Popovich A.F., Ral'chenko V.G., Cheshev E.A. *Kvantovaya Elektron*., **42** (11), 959 (2012) [*Quantum Electron*., **42** (11), 959 (2012)].
6. Bezotosnyi V.V., Bondarev V.Yu., Krokhin O.N., Oleshchenko V.A., Pevtsov V.F., Popov Yu.M., Cheshev E.A. *Tez. dokl. simp. 'Poluprovodnikovye lazery: fizika i tekhnologiya'* (Abstracts Symp. Semiconductor Lasers: Physics and Technology) (St. Petersburg, 2012) p. 14.
7. Nakwaski W. *Int. J. Optoelectron.*, **5** (5), 451 (1990).
8. Nakwaski W. *IEE Proc. I* , **131** (3), 94 (1984).
9. Nakwaski W. *Kvantovaya Elektron*., **11**, 391 (1984) [*Sov. J. Quantum Electron*., **14**, 266 (1984)].
10. Bezotosnyi V.V., Kumykov Kh.Kh., Markova N.V. *Kvantovaya Elektron*., **23** (9), 775 (1996) [*Quantum Electron*., **26** (9), 755 (1996)].
11. Bezotosnyi V.V., Kumykov Kh.Kh. *Kvantovaya Elektron*., **25** (3), 225 (1998) [*Quantum Electron*., **28** (3), 217 (1998)].